Published in final edited form as:
J Comp Neurol. 2009 August 1; 515(4): 454–464. doi:10.1002/cne.22078.

SELECTIVE REDUCTION OF NEURON NUMBER AND VOLUME OF THE MEDIODORSAL NUCLEUS OF THE THALAMUS IN MACAQUES FOLLOWING IRRADIATION AT EARLY GESTATIONAL AGES

Lynn D. Selemon[1,*], **Anita Begović**[1], and **Pasko Rakic**[1]

[1] Department of Neurobiology, Yale University School of Medicine, New Haven, CT 06520-8001

Abstract

Neurons in the macaque brain arise from progenitors located near the cerebral ventricles in a temporally segregated manner such that lethal doses of ionizing irradiation, if administered over a discrete time interval, can deplete individual nuclei selectively. A previous study showed that neuron number in the dorsal lateral geniculate nucleus is reduced following early gestational exposure to x- irradiation (Algan and Rakic, 1997). Here we examine whether similarly timed irradiation decreases neuron number in three associational thalamic nuclei: mediodorsal (MD), anterior, and pulvinar. Ten macaques were exposed to multiple doses of x-rays (total exposure: 175–350cGy) in early (E33-E42) or midgestation (E70-E90); 8 non-irradiated macaques were controls. Only the early irradiated monkeys, not the midgestationally irradiated animals, exhibited deficits in whole thalamic neuron (−15%) and glia numbers (−21%) compared to controls. Reduction of neuron number (−26%) and volume (−29%) was particularly pronounced in MD. In contrast, cell number and volume were not significantly decreased in the anterior or pulvinar nuclei following early gestational irradiation. Thus, reduced thalamic neuron number was associated specifically with irradiation in early gestation. Persistence of the thalamic neuronal deficit in adult animals indicates that prenatally deleted neurons had not been replenished during maturation or in adulthood. The selective reduction of MD neuron number also supports the protomap hypothesis that neurons of each thalamic nucleus originate sequentially from separate lines of neuronal stem cells (Rakic, 1977a). The early gestationally irradiated macaque is discussed as a potentially useful model for studying the neurodevelopmental pathogenesis of schizophrenia.

Keywords

anterior nucleus; pulvinar nucleus; neurodevelopment; stereology; schizophrenia

Systematic studies, based on injections of tritiated thymidine into pregnant macaque monkeys at different gestational ages, have established that each population of neurons in the developing primate brain is born, i.e., undergoes final mitotic division of the progenitor cells, during a specific and limited period (e.g. Rakic, 1974, 2002). For example, neurons destined to become the thalamus are born during the first trimester of pregnancy with neurogenesis in the dorsal lateral geniculate nucleus (dLGN) (E36-E43) having a similar although less prolonged duration than that of the pulvinar nucleus (E36-E45) (Rakic, 1977a;

Correspondence: Lynn D. Selemon, Ph.D., Department of Neurobiology, Yale University School of Medicine, PO Box 208001, New Haven, CT, 06520-8001, phone: 508-540-5306, fax: 508 540-5306, e-mail: ldselemon@aol.com.
Associate Editor: Joseph. L. Price

Ogren and Rakic, 1981). Neurogenesis in many other subcortical structures including the neostriatum (E36-E80), nucleus accumbens (E36-E85), septal nuclei (E36-E62), basal cholinergic nuclei (E33-E48), and brain stem monoaminergic nuclei (E27-E43), begins in early gestation and overlaps with thalamogenesis (Brand and Rakic, 1979, 1980; Levitt and Rakic, 1982; Kordower and Rakic, 1990). Genesis of neurons in the primary visual cortex begins slightly later and extends throughout the middle third (E45-E102) of the 165-day gestational period of the rhesus monkey (Rakic, 1974, 1977b).

The relatively prolonged period and temporal segregation of neurogenesis in the non-human primate is experimentally advantageous for deleting specific populations of neurons since populations that are in the final stages of mitosis are most vulnerable to the effects of ionizing irradiation. Algan and Rakic (1997) have previously shown that exposure of pregnant monkeys to multiple low doses of x-irradiation limited either to early (E33-E40) or midgestation (E70-E90) results in loss of neurons in the dorsal lateral geniculate nucleus and the primary visual cortex, respectively, in the offspring. More recently, *in vivo* magnetic resonance (MR) brain imaging was performed on monkeys that were prenatally exposed to x-irradiation and allowed to reach full adulthood. Analysis of the MR images indicated that volume of the whole thalamus was selectively reduced in monkeys irradiated during early gestation (E33-E42) compared to non-irradiated controls whereas midgestationally (E70-E82) irradiated monkeys had thalamic volumes indistinguishable from controls (Schindler et al., 2002). Interestingly, thalamic shape was altered in a non-uniform manner in the early irradiated group, suggesting that there might be inhomogeneity in volume reduction of individual thalamic nuclei (Schindler et al., 2002). Further analysis of cortical volumes in these same monkeys demonstrated the temporal specificity of the irradiation effects as monkeys irradiated in midgestation, but not in early gestation, showed significant reductions in cortical gray matter volume compared to controls (Selemon et al., 2005).

The present study was undertaken to determine whether exposure to x-irradiation in early gestation reduces the number of neurons in associational thalamic nuclei that have been prominently implicated in the pathology of schizophrenia (Pakkenberg, 1990; Young et al., 2000; Popken et al., 2000; Byne et al., 2001, 2002; Danos et al., 2003; Kemether et al., 2003). If thalamic number were reduced by early gestational exposure to irradiation, the fetally irradiated non-human primate could be used to model the thalamic pathology of schizophrenia and to examine the morphologic and behavioral sequelae consequent to prenatal elimination of thalamic neurons.

Materials and Methods

Subjects

Brains from 18 rhesus monkeys (*Macaca mulatta*) were examined in this study (Table 1). This total included 5 monkeys that were exposed to x-irradiation during the early fetal period (eFIMs), 5 monkeys exposed to fetal x-irradiation in midgestation (mFIMs) as an irradiated comparison group, and 8 non-irradiated control monkeys (CONs). Ten monkeys were sacrificed as adults (4.8–14.2 yrs); 8 monkeys were sacrificed as infants for a previous study of the visual system (Algan and Rakic, 1997).

In utero exposure to x-irradiation

Exposure to irradiation was performed according to the procedure previously reported in detail in Algan and Rakic (1997) and briefly described here. Pregnant monkeys were sedated with ketamine (5–10 mg/kg) and restrained with atropine (0.02 mg/kg). Ultrasound was used to locate the head of the fetus and to estimate the depth of the head from the abdominal surface. A 250 kV, 15 mA Stabilipan x-ray tube was used to deliver a beam of irradiation

(area 5× 5 cm) to the head of the fetus. Depth of the head was taken into account in determining the duration of the exposure necessary to achieve the target dose of irradiation. Exposure dose varied from 50–100 cGy; exposure to irradiation was repeated generally every other day for a total of 3–7 exposures totally 175–350 cGy (Table 1). The higher exposure dosages were administered in midgestation. Exposure during the period of thalamogenesis was not greater than 200 cGy (Table 1). Following irradiation, the status of the pregnant monkeys was monitored by ultrasound every two weeks for the remainder of the gestational period. The irradiated offspring were delivered by Caesarian section at term (E165) and were raised in the nursery until approximately 6 months of age when they were transferred to the adult colony. All animals in this study were housed, fed, and sacrificed according to protocols approved by Yale's Institutional Animal Care and Use Committee.

Histological processing of brains

Monkeys were sedated with ketamine and then deeply anesthetized with sodium pentobarbital. The animals were perfused intracardially with 1.5–2.0 liters of 0.1M phosphate buffered saline (pH = 7.4; room temperature) followed by 3–4 liters of a mixed aldehyde fixative (4 % paraformaldehyde + 0.2 % glutaraldehyde in 0.1M phosphate buffer at 4°C). Following fixation, the brains were removed, and the left thalamus was dissected in one large block. Smaller blocks of the right hemispheres were dissected for non-stereologic analyses not reported here. The thalamic block was embedded in celloidin and sectioned coronally at 40 μm on a sliding microtome. A 1-in-20 series of sections was collected and stained with a standard Nissl stain (cresyl violet) for cytoarchitectonic delineation of thalamic nuclei and for stereologic analyses. The thalamic block from one early irradiated infant monkey (eFIM5, see Table 1) did not include the entire posterior thalamus and therefore analysis was limited to MD and the anterior nucleus in this animal.

Stereologic analysis of total cell number

All stereologic analyses were conducted by viewing the sections on a Zeiss Axioskop microscope which had been fitted with an integrated, computer-guided Neurolucida system, including a motorized stage, linear z-axis recorder, and Stereo Investigator (ver. 5.05) software (MicroBrightfield, Williston, VT). All analyses were performed blind to diagnostic status by a single observer (AB).

The total number of neurons and glia in the whole thalamus, as well as in the mediodorsal (MD), anterior, and pulvinar nuclei, was estimated using the optical disector method (Gundersen, 1986). Systematic, random sampling was achieved by applying the fractionator method which involved grid-based sampling with optical disectors in every 20th section through the entire thalamus or nucleus of interest (Gundersen 1986). Contours of the area of interest were drawn at low power (90x; 2.5x air objective, numerical aperature = 0.075), and cells were counted under high power (3600x; 100x oil immersion objective; numerical aperature = 1.30).

Section thickness was measured on slide, and differences in z-axis shrinkage between groups for the whole thalamus and for each of the three nuclei were examined with an ANOVA with posthoc comparisons corrected for multiple comparisons with a Bonferroni adjustment. For example, mean section thickness for the whole thalamus (CON= 35.3μm (range 33.7–36.1), eFIM=33.7 μm (range 32.4–35.8), mFIM= 34.7 μm (range 32.3–38.5)) revealed that histological processing was associated on average with 12% z-axis shrinkage (range 8.45%–15.75%). No significant differences between groups were found. Comparison of adult and infant section thicknesses for each region of interest was tested via a Student's t-test. Mean section thickness for adults versus infants for whole thalamus (adults= 34.8 μm

(range 33.1–36.0); infants=34.7 μm (range 32.3–38.5)) and for the three individual nuclei were not significantly different.

Prior to the actual analysis, optimal parameters for disector size and sampling grid spacing were determined. Thus, an optical disector dimension of 58 (l) × 50 (w) × 25 (h) μm was chosen to maximize the size of the disector but still allow for ≥2 μm guard zones at the top and bottom of the section. The guard zones chosen allowed the top and bottom of the box to be sufficiently distant from the section top and bottom edges in order that lost caps, warping, and irregularities associated with these parts of the section were not included in the optical disector. This was confirmed by observation under the microscope during the pilot study. A pilot study was performed to determine the grid spacing for the whole thalamus and individual nuclei that would yield a sampling coefficient of error (CE) ≤ 0.05 for each structure (Gundersen et al., 1999). Optimal sampling grid sizes were 800 μm × 1200 μm for the whole thalamus, 300 μm × 600 μm for the mediodorsal and pulvinar nuclei, and 150 μm × 150 μm for the anterior nucleus. Mean CEs for the whole thalamus, MD, and pulvinar nuclei were 0.03 (neurons) and 0.02 (glia); mean CEs for theanterior nucleus were 0.04 (neurons) and 0.03 (glia).

In each section, the contours of the whole thalamus or individual thalamic nuclei were traced at low power under a 2.5x objective. Sections were then examined under a high power, 100x oil immersion objective. Neurons containing a nucleus that was in focus inside the optical disector were counted; glial nuclei inside the disector were counted as well. Neurons were distinguished from glia on the basis of morphologic characteristics of the nucleus including clumping of chromatin and sharper delineation of the nuclear membrane in glia as illustrated previously (Selemon et al., 1999). The optical disector/optical fractionator probe utilizes unbiased counting frames to ensure unbiased subsampling in the region of each optical disector.

Stereologic analysis of volume

The estimate of volume generated by the optical fractionator probe, based on contour outlines, was used for whole thalamus and for individual thalamic nuclei. The accuracy of this estimate was verified by re-measuring volume of all the adult animal probes using a point-counting based version of the Cavalieri method (Gundersen et al., 1988) at low power (2.5X objective). The area associated with each point was 2500 μm^2. Mean number of points counted was 86,418 (range 74,933–121,181) for whole thalamus, 16,186 (range 11,737–20,697) for MD, 2,244 (range 1950–2998) for the anterior nucleus and 30,554 (range 14,860–44,984) for the pulvinar nucleus. Mean CEs for volume measurements generated by the optical fractionator probe were 0.03 (whole thalamus), 0.04 (MD), 0.09 (anterior nucleus), and 0.06 (pulvinar nucleus); mean CEs for volume measurements based on point counting were 0.006 (whole thalamus), 0.008 (MD), 0.02 (anterior nucleus), and 0.012 (pulvinar nucleus). Mean differences between measures were 2.2 mm^3 (whole thalamus), 0.5 mm^3 (MD), 0.09 mm^3 (anterior nucleus) and 1.0 mm^3 (pulvinar nucleus).

Statistical methods

Statistics were performed using SPSS (ver. 15.0). Regression analysis was performed on the control brains to assess the effect of age on cell number and volume. Significant effects of age on whole thalamic neuron ($r= -0.651$, $p= 0.041$) and glia number ($r= -0.902$, $p\leq 0.001$), as well as MD neuron ($r= -0.670$, $p= 0.034$) and glia number ($r= -0.701$, $p= 0.035$), were observed. Neuron and glia number in the pulvinar and anterior nuclei did not show a significant relationship with age (all $r < 0.44$. all $p> 0.24$). Interestingly, neither volume of the whole thalamus, nor volume of individual nuclei, was significantly correlated with age (all $r< 0.45$, all $p> 0.23$). Nonetheless, all analyses of group effects were performed using a

univariate analysis of covariance (ANCOVA) with age as the covariate. Post-hoc comparisons between groups were performed with a Bonferroni correction to account for multiple comparisons. All data are expressed as mean ± standard error of the mean.

Photography/image adjustment

For Figure 1, selected slides were scanned on an Aperio ScanScope at 20x magnification. High power views of neurons in Figure 2 were photographed with a Nikon Cool Pix 990 camera. Images were transferred to Adobe Photoshop, ver. 8.0, for conversion to gray scale and adjustment of brightness and contrast. The photomicrographs were then assembled into figures in Canvas, ver 9.0.4, and labels and nuclear outlines were added.

Results

Delineation of thalamic borders

Cytoarchitectonic determination of thalamic borders was based on the online atlas of the macaque brain at BrainMaps.org. The nomenclature of this atlas will be used to describe the borders and the nuclei of the thalamus (Fig. 1). At the most anterior level of the thalamus (not shown), the medial border of thalamus is formed by the third ventricle while the ventral, lateral and dorsal borders of the thalamus are constituted by the hypothalamus, the internal capsule and stria medullaris and fornix, respectively. At slightly more posterior levels, the thalami of the two hemispheres are joined at the midline and therefore, the midline defines the medial border (Fig. 1A,B). More posteriorly, the zona incerta extends from the reticular nucleus of the thalamus to form a portion of the ventral boundary (Fig 1C,D). Note that the lateral geniculate nucleus, which is located apart from the main body of the thalamus at this level, was included in measurements of whole thalamic volume and cell number. Far posteriorly, the pulvinar and reticular nuclei are the only thalamic nuclei present and they are bordered laterally by the white matter bundles of the parietal lobe, the tail of the caudate and the fornix (Fig. 1E,F).

Neurons in MD (Fig. 2A), anterior (Fig. 2B) and pulvinar (Fig. 2C) nuclei were large, elongated cells with pale nuclei and well defined nucleoli. The predominant glial type was a small, round nucleus with multiple clusters of heterochromatin and no visible cytoplasm (Fig. 2).

Thalamic total cell number

The thalamus extended over an average of 10.8 sections (range 10–13); 273 sites (range 217–367) were sampled, and 1200 neurons (range 996–1336) and 2894 glia (range 1797–3861) were counted. There was a significant effect of group on whole thalamic neuron number ($F_{1,2}$= 6.488, p= 0.011) and glia number ($F_{1,2}$= 6.619, p= 0.01). Posthoc comparison of adjusted group means revealed that there were fewer neurons in the eFIM group in comparison to CONs and to mFIMs (Table 2, Fig. 3). Likewise, glia number was reduced in eFIMs relative to CONs and to mFIMs (Table 2, Fig. 3).

In the MD nucleus, which extended over 7.4 sections (range 7–9), 281 sites (range 184–384) were sampled, and 1159 neurons (range 742–1390) and 2196 glia (range 1325–2940) were counted. Univariate ANCOVA revealed a significant effect of group on number of neurons in the MD nucleus ($F_{1,2}$= 4.251, p= 0.036) but no group effect for glia number ($F_{1,2}$= 2.327, p= 0.134). Posthoc comparison of mean neuron number indicated that eFIMs had fewer MD neurons than CONs, whereas mFIMs did not differ from CONs nor from eFIMs (Table 2, Fig. 4).

The anterior nucleus extended through 7 sections in all brains. An average of 215 optical disectors (range 173–253) yielded 806 neurons (range 584–1046) and 1318 glia (range 1014–1596). A significant group effect was observed for neuron number in the anterior nucleus (neurons: $F_{1,2}$= 3.765, p= 0.049) with posthoc comparisons revealing a marginally significant difference (p=.08) between group means for eFIMs in comparison to mFIMs (Table 2, Fig. 4). Glia number did not differ between groups ($F_{1,2}$= 1.233, p= 0.321).

An average of 523 sites (range 372–685) were sampled in the pulvinar nucleus in 7.2 sections (range 5–9), and 1715 neurons (range 1182–1974) and 3221 glia (range 2081–3959) were counted. In the pulvinar, there was a significant effect of group on neuron number ($F_{1,2}$=3.800, p= 0.05) although only a trend difference (p.07) was observed between eFIM and mFIM means (Table 2, Fig. 4). Glia number did not differ between groups in the pulvinar nucleus ($F_{1,2}$= 0.154, p= 0.859).

Thalamic volume

Whole thalamic volume did not differ between groups ($F_{1,2}$= 2.326, p=0.137). However, MD volume showed a significant group effect ($F_{1,2}$= 5.275, p= 0.02). Post-hoc comparison of MD volumes between groups indicated that eFIM volume was smaller than CONs (Table 2, Fig. 5). MD volume in mFIMs did not differ significantly from either CONs or eFIMS (Table 2, Fig. 5). Significant group effects were not observed for volume of the anterior ($F_{1,2}$= 1.799, p= 0.202) or pulvinar nuclei ($F_{1,2}$= 1.964, p= 0.180) (Table 2, Fig. 5).

Discussion

Reduction of thalamic cell number and volume was observed in monkeys that had been exposed to irradiation in early gestation (E33-E42) whereas fetal irradiation in midgestation (E70-E90) did not result in any discernible thalamic pathology. These findings indicate that only structures that are in the process of neurogenesis undergo pronounced cell loss due to the lethal effects of irradiation on dividing cell populations and that neurons generated before or after irradiation are not affected (Rakic, 1977a; Algan and Rakic, 1997; Schindler et al., 2002; Selemon et al., 2005). The observed decrease in neuron and glia number in the whole thalamus of early gestationally irradiated animals suggests that the impact of prenatal irradiation is widespread throughout the thalamus. However, significant reductions in neuron number and volume were observed only in the MD nucleus and not in the anterior or pulvinar nuclei. These findings indicate that among of the three nuclei studied, the MD nucleus is particularly vulnerable to the effects of irradiation during the early gestational period targeted in this study which could be due to the technical or biological reasons. These results in general support the notion that individual thalamic nuclei are generated from distinct neuronal precursors and therefore can be affected differentially by environmental factors (Rakic, 1977a, 1988, 2002). They are also in harmony with the recent discoveries that laminar and phenotypic specificity of cortical neurons can be traced to separate neuronal progenitors in the ventricular zone (Chen et al., 2005a,b; Choflin and Rubenstein, 2007; Dominguez and Rakic, 2008; Molyneaux et al., 2005; O'Leary and Borngasser, 2006).

Technical comments

The number of adult animals available for quantitative analysis was relatively small because of the difficulties in obtaining the timed pregnancies and the lengthy experimental period necessary to generate adult animals that have been exposed to irradiation *in utero*. We therefore analyzed the thalamus of several infant monkeys; all were previously included in the Algan and Rakic (1997) study. Although it is well established that all neurons in the macaque thalamus are generated prenatally, generation of neurons is not the only factor in determining final number. Neurons in the thalamus, as in most brain regions, are

overproduced, and the excess neurons are eliminated during maturational processes (Williams and Rakic, 1988; Oppenheim, 1991; Lotto et al., 2001; Abitz et al., 2007). Indeed, neuron number in the thalamus as a whole and in the MD nucleus exhibited a significant inverse correlation with age, suggesting that postnatal neuronal pruning may have occurred. However, the effect of age was taken into account by the statistical analyses that incorporated age as a covariate in the ANCOVA.

The age range in the subject group also extended into the early teens; the adult monkeys in this study ranged in age from 4.8 to 14.2 years of age. However, this age range does not extend beyond normal, full maturity. Rhesus monkeys (*Macaca mulatta*) can live as long as 40 years in captivity and do not show signs of aging until they are in their late teens (Tigges et al., 1988). These observations concur with measurements of volume and cell number in the thalamus in the present study as neither of these parameters was decreased in the two young teenaged, control monkeys. Moreover, the adult monkey that was irradiated in midgestation, though older than the early gestationally irradiated, exhibited thalamic morphology that was indistinguishable from the normal young adult controls.

There was also variability in the timing and dose of irradiation exposure across animals in the two irradiated groups. The non-uniformity of the exposure may be attributed to several factors including uncertainty in the exact onset of pregnancy (~± 2 days), differences in dates of exposure, and variability in location of the head of the fetus in the mother's abdomen. Individual biological variability may also have contributed as there were sizeable standard deviations for the nonirradiated control groups as well. Monkeys exposed to irradiation in midgestation received higher doses of radiation that those exposed in early gestation. Despite the more prolonged and intense irradiation in the midgestationally irradiated animals, measurements of volume and cell number of the thalamus did not reveal any abnormalities. Therefore, the pathologic effects of radiation cannot simply be related to dosage. The timing of radiation exposure and relationship of that exposure period to the time of neurogenesis are most critical in determining which brain structures will exhibit a reduction in cell number and volume. Because neurogenesis in the thalamus was complete before the midgestational period of irradiation in these animals, the adverse effects of ionizing radiation on dividing cells did not affect the thalamus.

Whole brain volume or whole brain weight was not available for the monkeys included in this study. In our previous MR study of thalamic volume in adult irradiated monkeys, including the 3 adult eFIMS in this study, reductions in thalamic volume were significant only after variations in whole brain volume were taken into account (Schindler et al., 2002). It is therefore possible that our failure to find significant differences in whole thalamic volume in this study may be related to individual variations in whole brain size. Indeed, volume differences in postmortem studies are confounded not only by biologic variation but also by differences in shrinkage due to postmortem processing.

Number weighted counts, i.e., counts adjusted for section thickness (Dorph-Petersen et al., 2001), were not used in this study. However, it seems unlikely that differences in shrinkage of tissue in the z-axis influenced the results. Measurements of mean section thickness did not reveal any differences between groups. Furthermore, differential shrinkage in the z-axis was not found when measurements from infant and adults were compared. Our observations are in accordance with a stereologic study of MD in infant and adult humans that also did not find age-related variation in z-axis shrinkage in paraffin embedded sections (Abitz et al., 2007).

Reductions in neuronal number and volume limited to MD

Of the three nuclei examined in the present study, only MD showed significant reductions in total neuron number following early gestational irradiation. One possibility for this selective vulnerability is that the period of irradiation exposure chosen in this study most closely matches the peak period of neurogenesis for MD and conversely does not coincide as well with the peak of neurogenesis for the anterior and pulvinar nuclei. Previously, Algan and Rakic (1997) have reported that irradiation exposure during this same period, including many of the same animals examined in this study, reduced neuron number in the dLGN. Notably, neurogensis in the pulvinar nucleus (E36-E45) extends for 2 days longer than neurogenesis in the dLGN (E36-E43), perhaps indicating that peak neurogeneis in the pulvinar may occur slightly later than that of the dLGN. Whether slight differences in peak neurogenesis can account for the more pronounced depletion of neurons in MD is speculative at this point because precise data on time and duration of neurogenesis, as well as kinetics of proliferation, are not available for the MD in primates. However, in studies in rats in which neurogenesis is compressed by the much shorter gestational duration, birthdates of individual thalamic nuclei are slightly staggered as, for example, the anterior and mediodorsal nuclei are generated a day or two later than the primary sensory relay nuclei (Altman and Bayer, 1979, 1988). Moreover, different classes of neurons within a nucleus may be generated sequentially. For example, within the dLGN of the macaque, early generated cells migrate to a position within the ventrally situated magnocellular layers whereas later generated neurons lie within the more dorsal parvocellular layers (Rakic, 1977a).

Finally, competition between neurons for survival could account for the apparent neuronal loss in MD but not in anterior or pulvinar nuclei. A basic tenet of neurodevelopment is that neurons, as well as projections and synapses, are produced in exuberance and that the excess numbers are pruned back to adult levels by competition (Rakic et al., 1986; Oppenheim, 1991; Innocenti and Price, 2005). For example, it has been shown that when one eye is enucleated in the monkey embryo, the other eye will then have a much larger number of optic axons in the adult, presumably because it retains overproduced axons in the absence of the competition from the contralateral enucleated eye (Rakic and Riley, 1983). Similarly, survival of dorsal thalamic neurons is dependent on levels of brain derived neurotrophic factor (BDNF) in their target cortical areas, perhaps providing a mechanism to ensure that the proper proportion of thalamic and cortical neurons is established (Lotto et al., 2001). Such competition for cortical target sustenance may play a part in determining final neuron number in MD, anterior and pulvinal nuclei, and since these associational nuclei have multiple reciprocal connections with widespread areas of cortex, as well as connections with subcortical areas, it is difficult to predict how the relative sizes and synaptic weights of the connections will ultimately influence neuron number.

Given the relatively small sample size, the lack of significant effect of the radiation on the anterior and pulvinar nuclei must be interpreted cautiously. Mean volumes of the anterior and pulvinar nuclei for the early gestationally irradiated animals were decreased to the same magnitude as in MD (pulvinar nucleus: −24%; anterior nucleus: −15%) suggesting that individual variability accounted for the lack of significance. Moreover, neuron number exhibited a trend decrease in the early compared to the midgestationally irradiated monkeys in these nuclei, again suggesting that a deficit in neuron number in these nuclei might have emerged with a larger sample size.

Relationship to in vivo imaging findings in irradiated monkeys

The adult irradiated monkeys in this study, i.e., 3 early gestationally irradiated and 1 midgestationally irradiated, have previously undergone structural MR imaging in collaboration with Csernansky and colleagues (Schindler et al., 2002; Selemon et al., 2005). High dimensional diffeomorphic brain mapping (Miller et al.., 1993, 1997) of the thalamus revealed that early gestational irradiation results in a reduction of thalamic volume (~25%) that while slightly larger is nonetheless comparable to the volumetric deficit (15%), albeit non-significant, measured in this postmortem study using stereologic methods (Schindler et al., 2002). It should be noted that there was only partial overlap of controls and early irradiated monkeys between this study and the neuroimaging analysis. As reported here, monkeys that were irradiated during midgestation did not exhibit reduced thalamic volume compared to non-irradiated controls (Schindler et al., 2002). Moreover, in the early irradiated group, thalamic shape was altered in a non-homogeneous manner, with the posterior thalamus showing more marked inward deformation than the anterior thalamus (Schindler et al., 2002). In the present postmortem analyses of these animals, there was considerable variability in the deleterious effects of radiation on individual thalamuc nuclei. The MD nucleus exhibited the most pronounced cytoarchitectural deficits, showing a 29% reduction in volume and 26% reduction in total neuron number. While selective involvement of MD nucleus was not apparent from the pattern of shape deformation observed from structural imaging, this might be due to the limited extent to which MD forms a surface of the thalamus or may indicate that reduction of volume in any given nucleus can result in distortion of thalamic shape at surfaces remote from the site of volumetric atrophy. Further studies comparing *in vivo* maps of inward deformation in individual animals with postmortem measures in the same animal are needed to clarify the relationship between the imaging and stereologic data.

Cortical volumes were also assessed from high resolution magnetic resonance scans of the irradiated monkeys. In marked contrast to the findings in thalamus, monkeys that had been exposed to irradiation in midgestation had significant reductions in gray matter volume in both frontal and non-frontal cortical areas whereas gray matter volumes in early gestationally irradiated monkeys did not differ from controls (Selemon et al., 2005). These data showing a double dissociation between thalamic and cortical volume in the two irradiated groups reaffirms that the precise timing of irradiation determines which brain regions are impacted by the irradiation. Thalamic neurons are generated in early gestation and are therefore directly impacted by the irradiation at E33-E42 while midgestational irradiation presumably eliminates a large proportion of developing cortical neurons and results in reduced gray matter volume. Notably, irradiation at either time point produces a sizeable reduction in cortical white matter volume (Selemon et al., 2005), indicating that cortical connections are diminished as the result of either subcortical or cortical neuronal loss.

Relevance to schizophrenia

One of the most prominent neuropathologic features of the schizophrenic brain is reduced volume and neuron number of the thalamus. Neuroimaging studies have revealed reductions in volume (Andreasen et al., 1994; Buchsbaum et al., 1996; Gur et al., 1998; Gilbert et al., 2001) and shape of the whole thalamus (Hazlett et al., 1999; Csernansky et al., 2004), and volume of individual thalamic nuclei (Byne et al., 2001; Kemether et al., 2003) and of thalamocortical tracts (Andreasen et al., 1994). Stereologic analyses in postmortem brains from schizophrenic subjects have shown that neuron number is reduced in associational nuclei, including MD, the anterior and pulvinar nuclei (Pakkenberg, 1990; Young et al., 2000; Popken et al., 2000; Danos et al., 2003, 2003). Admittedly, there are a number of

studies that have not uncovered thalamic pathology in schizophrenia (Portas et al., 1998; Arciniegas et al., 1999; Cullen et al., 2003; Dorph-Petersen et al., 2004; Young et al., 2004; Danos et al., 2005; Preuss et al., 2005; Kreczmanski et al., 2007; Nielsen et al., 2008); however, the weight of evidence suggests that reduced neuronal number is an important structural anomaly that distinguishes at least a subset of schizophrenic subjects from individuals without psychiatric illness.

In addition, there is a wealth of evidence supporting a neurodevelopmental origin for schizophrenia. Prenatal stressors, including maternal malnutrition, maternal infection, and rH incompatibility, have been associated with an increased incidence of schizophrenia in affected populations (Mednick et al., 1988; Susser and Lin, 1992; Susser et al., 1996; Hollister et al., 1996; Brown et al., 2000), and interestingly, preliminary evidence suggests that exposure to diagnostic x-ray during pregnancy results in an elevated incidence of schizophrenia spectrum disorders in male progeny (R. Gross, personal communication). Most often the critical period for developmental perturbation has been identified as either the first or second trimester of gestation. These studies suggest that disruption of early developmental processes may be responsible for the pattern of pathology that has been identified in brains of schizophrenic subjects. The present study indicates that reduction of thalamic neuron number and volume in schizophrenia could have an early gestational origin.

Prenatal exposure to radiation in humans

Human populations have been exposed to high doses of radiation following two tragic events, the Japanese bombings at the close of World War II and the more recent 1986 Chernobyl nuclear plant accident. Fetal exposure to the atomic bombings at 8–25 weeks gestation has been shown to have profound effects on brain development such that exposed individuals exhibited severe mental retardation, an increase in seizure disorders, and decreased head size (for review, see Otake et al., 1991). Although fetal exposure to irradiation in this Japanese population has not been associated with an increase in schizophrenia or other neuropsychiatric disorders, it could be that atomic radioactivity which is more damaging to human tissues than x-rays, causes severe global brain impairment manifesting as mental retardation rather than mental illness. In contrast, the more recent prenatal exposure following the Chernobyl disaster has resulted in a wide range of neurologic disorders in children who were examined at 11–13 years of age (Loganovskaja and Loganovsky, 1999; Loganovsky et al., 2008). These prenatally exposed individuals exhibit decreased full and verbal IQ, disorganized EEG patterns and other signs of abnormal functioning of the left hemisphere. Notably, individuals exposed *in utero* to the Chernobyl radiation are only now passing through the critical age on onset for schizophrenia. Adult survivors of the Chernobyl accident who were exposed to moderate to high levels of radiation have an increased expression of left frontotemporal limbic dysfunction and schizophreniform disorders (Loganovsky and Loganovskaja, 2000). Thus, these findings suggest that human exposure to ionizing radiation may be associated with compromise of the left frontotemporal axis that could predispose individuals to schizophrenia.

Supplementary Material

Refer to Web version on PubMed Central for supplementary material.

Acknowledgments

We would like to recognize the contribution of Dr. Oguz Algan for experimental treatment of the irradiated monkeys in this study. We also thank Heidi Voegeli, Heather Findlay, and Marianne Horn for excellent technical assistance.

Supported by RO1-MH 59329 (LDS), P50-MH44866 (Patricia S. Goldman-Rakic, Ph.D., Program Director), P50-MH 71616 (John G. Csernansky, M.D./Deanna M. Barch, Ph.D., Program Directors), NY-014841 (PR), and EY-02593 (PR).

Abbreviations

3V	third ventricle
A	anterior nucleus
CA	caudate nucleus
CC	corpus callosum
CeM	central medial nucleus
CL	central lateral nucleus
CM	centre median nucleus
F	fornix
GP	globus pallidus
HPT	habenulopeduncular tract
IC	internal capsule
LD	lateral dorsal nucleus
LGd	dorsal lateral geniculate nucleus
LP	lateral posterior nucleus
MD	mediodorsal nucleus
MG	medial geniculate nucleus
MV	medioventral nucleus
Pa	paraventricular nuclei
Pc	paracentral nucleus
Pf	parafascicular nucleus
Pl	pulvinar
Pul	putamen
R	reticular nucleus
SM	stria medullaris
VA	ventral anterior nucleus
VLa	ventral lateral anterior nucleus
VLp	ventral lateral posterior nucleus
VM	ventral medial nucleus
VPL	ventral posterior lateral nucleus
ZI	zona incerta

Literature Cited

Abitz M, Damgaard Nielsen R, Jones EG, Laursen H, Graem N, Pakkenberg B. Excess of neurons in the human newborn mediodorsal thalamus compared with that of the adult. Cereb Cortex. 2007; 17:2573–2578. [PubMed: 17218480]

Algan O, Rakic P. Radiation-induced, lamina-specific deletion of neurons in the primate visual cortex. J Comp Neurol. 1997; 12:335–352. [PubMed: 9133572]

Altman J, Bayer SA. Development of the diencephalon in the rat. IV. Quantitative study of the time of origin of neurons and the internuclear chronological gradients in the thalamus. J Comp Neurol. 1979; 188:455–471. [PubMed: 489803]

Altman J, Bayer SA. Development of the rat thalamus: II. Time and site of origin and settling pattern of neurons derived from the anterior lobule of the thalamic neuroepithelium. J Comp Neurol. 1988; 275:378–405. [PubMed: 3225344]

Andreasen NC, Arndt S, Swayze V II, Cizadlo T, Flaum M, O'Leary D, Ehrhardt JC, Yuh WTC. Thalamic abnormalities in schizophrenia visualized through magnetic resonance image averaging. Science. 1994; 266:294–298. [PubMed: 7939669]

Arciniegas D, Rojas DC, Teale P, Sheeder J, Sandberg E, Reite M. The thalamus and the schizophrenia phenotype: failure to replicate reduced volume. Biol Psychiatry. 1999; 45:1329–1335. [PubMed: 10349040]

Brand S, Rakic P. Genesis of the primate neostriatum: [^{3}H]thymidine autoradiographic analysis of the time of neuron origin in the rhesus monkey. Neuroscience. 1979; 4:767–778. [PubMed: 113693]

Brand S, Rakic P. Neurogenesis of the nucleus accumbens septi and neighboring septal nuclei in the rhesus monkey: A combined [^{3}H]thymidine and electron microscopic study. Neuroscience. 1980; 5:2125–2138. [PubMed: 7465048]

Brown AS, Schaefer CA, Wyatt RJ, Geotz R, Begg MD, Gorman JM, Susser ES. Maternal exposure to respiratory infections and adult schizophrenia spectrum disorders: a prospective birth cohort study. Schizophr Bull. 2000; 26:287–295. [PubMed: 10885631]

Buchsbaum MS, Someya T, Teng CY, Abel L, Chin S, Najafi A, Haier RJ, Wu J, Bunney WE Jr. PET and MRI of the thalamus in never-medicated patients with schizophrenia. Am J Psychiatry. 1996; 153:191–199. [PubMed: 8561198]

Byne W, Buchsbaum MS, Kemether E, Hazlett EA, Schinwari A, Mitropoulou V, Siever LJ. Magnetic resonance imaging of the thalamic mediodorsal nucleus and pulvinar in schizophrenia and schizotypal personality disorder. Arch Gen Psychiatry. 2001; 58:133–140. [PubMed: 11177115]

Byne W, Buchsbaum MS, Mattiace LA, Hazlett EA, Kemether E, Elhakem SL, Purohit DP, Haroutunian V, Jones L. Postmortem assessment of thalamic nucleuar volumes in subjects with schizophrenia. Am J Psychiatry. 2002; 159:59–65. [PubMed: 11772691]

Chen B, Schaevitz LR, McConnell SK. Fezl regulates the differentiation and axon targeting of layer 5 subcortical projection neurons in cerebral cortex. Proc Natl Acad Sci USA. 2005a; 102:17184–17189. [PubMed: 16284245]

Chen JG, Rasin MR, Kwan KY, Sestan N. Zfp312 is required for subcortical axonal projections and dendritic morphology of deep-layer pyramidal neurons of the cerebral cortex. Proc Natl Acad Sci USA. 2005b; 102:17792–17797. [PubMed: 16314561]

Cholfin JA, Rubenstein JLR. Patterning of frontal cortex subdivisions by Fgf17. Proc Natl Acad Sci USA. 2007; 104:7652–7657. [PubMed: 17442747]

Csernansky JG, Schindler MK, Splinter NR, Wang L, Gado M, Selemon LD, Rastogi-Cruz D, Posener JA, Thompson PA, Miller MI. Abnormalities of thalamic volume and shape in schizophrenia. Am J Psychiatry. 2004; 161:896–902. [PubMed: 15121656]

Cullen TJ, Walker MA, Parkinson N, Craven R, Crow TJ, Esiri MM, Harrison PJ. A postmortem study of the mediodorsal nucleus of the thalamus in schizophrenia. Schizophr Res. 2003; 60:157–166. [PubMed: 12591579]

Danos P, Baumann B, Bernstein H-G, Stauch R, Krell D, Falkai P, Bogerts B. The ventral lateral posterior nucleus of the thalamus in schizophrenia: a post-mortem study. Psychiatry Res Neuroimag. 2002; 114:1–9.

Danos P, Baumann B, Karamer A, Bernstein H-G, Stauch R, Krell D, Falkai P, Bogerts B. Volumes of association thalamic nuclei in schizophrenia: a postmortem study. Schizophr Res. 2003; 60:141–155. [PubMed: 12591578]

Danos P, Schmidt A, Baumann B, Bernstein HG, Northoff G, Stauch R, Krell D, Bogerts B. Volume and neuron number of the mediodorsal thalamic nucleus in schizophrenia: a replication study. Psychiatry Res. 2005; 140:281–289. [PubMed: 16297604]

Dominguez MH, Rakic P. Neuroanatomy of the FGF system. J Comp Neurol. 2008; 509:141–143. [PubMed: 18459136]

Dorph-Petersen KA, Nyengaard JR, Gundersen HJG. Tissue shrinkage and unbiased stereological estimation of particle number and size. J Microscopy. 2001; 204:232–246.

Dorph-Petersen KA, Pierri JN, Sun Z, Sampson AR, Lewis DA. Stereological analysis of the mediodorsal thalamic nucleus in schizophrenia: volume, neuron number, and cell types. J Comp Neurol. 2004; 472:449–462. [PubMed: 15065119]

Gilbert AR, Rosenberg DR, Harenski K, Spencer S, Sweeney JA, Keshavan MS. Thalamic volume in patients with first-episode schizophrenia. Am J Psychiatry. 2001; 158:618–624. [PubMed: 11282698]

Gundersen HJG. Stereology of arbitrary particles. A review of unbiased number and size estimators and the presentation of some new ones, in memory of William R. Thompson. J Microsc. 1986; 143:3–45. [PubMed: 3761363]

Gundersen HJG, Jensen EBV, Kieû K, Nielsen J. The efficiency of systematic sampling in stereology reconsidered. J Microsc. 1999; 193:199–211. [PubMed: 10348656]

Gundersen HJG, Bendtsen TF, Korbo L, Marcussen N, Moller A, Nielsen K, Nyengaard JR, Pakkenberg B, Sorensen FB, Vesterby A, West MJ. Some new, simple and efficient stereological methods and their use in pathological research and diagnosis. Acta Pathol Microbiol Immunol Scand. 1988; 96:379–394.

Gur RE, Maany V, Mozley PD, Swanson C, Bilker W, Gur RC. Subcortical MRI volumes in neuroleptic naïve and treated patients with schizophrenia. Am J Psychiatry. 1998; 155:1711–1717. [PubMed: 9842780]

Hazlett EA, Buchsbaum MS, Byne W, Wei T-C, Speigel-Cohen J, Geneve C, Kinderlehrer R, Haznedar MM, Shihabuddin L, Siever LJ. Three-dimensional analysis with MRI and PET of the size, shape, and function of the thalamus in the schizophrenia spectrum. Am J Psychiatry. 1999; 156:1190–1199. [PubMed: 10450259]

Hollister JM, Laing P, Mednick SA. Rhesus incompatibility as a risk factor for schizophrenia in male adults. Arch Gen Psychiatry. 1996; 53:19–24. [PubMed: 8540773]

Innocenti GM, Price DJ. Exuberance in the development of cortical networks. Nat Rev Neurosci. 2005; 6:955–965. [PubMed: 16288299]

Kemether EM, Buchsbaum MS, Byne W, Hazlett EA, Haznedar M, Brickman AM, Platholi J, Bloom R. Magnetic resonance imaging of mediodorsal, pulvinar, and centromedian nuclei of the thalamus in patiens with schizophrenia. Arch Gen Psychiatry. 2003; 60:983–991. [PubMed: 14557143]

Kreczmanski P, Heinsen H, Mantua V, Woltersdorf F, Masson T, Ulfig N, Schmidt-Kastner R, Korr H, Steinbusch HW, Hof PR, Schmitz C. Volume, neuron density and total neuron number in five subcortical regions in schizophrenia. Brain. 2007; 130:678–692. [PubMed: 17303593]

Kordower JH, Rakic P. Neurogenesis of the magnocellular basal forebrain nuclei in the rhesus monkey. J Comp Neurol. 1990; 291:637–653. [PubMed: 2329194]

Levitt P, Rakic P. The time of genesis, embryonic origin and differentiation of the brain stem monoamine neurons in the rhesus monkey. Develop Brain Res. 1982; 4:35–57.

Loganovskaja TK, Loganovsky KN. EEG, cognitive and psychopathological abnormalities in children irradiated *in utero*. Int J Psychophysiol. 1999; 34:213–224. [PubMed: 10610046]

Loganovsky KN, Loganovskaja TK. Schizophrenia spectrum disorders in persons exposed to ionizing radiation as a result of the Chernobyl accident. Schizophr Bull. 2000; 26:751–773. [PubMed: 11087010]

Loganovsky KN, Loganovskaja TK, Nechayev SY, Antipchuk YY, Bomko MA. Disrupted development of the dominant hemisphere following prenatal irradiation. J Neuropsychiatry Clin Neurosci. 2008; 20:274–291. [PubMed: 18806231]

Lotto RB, Asavaritikra P, Vali L, Price DJ. Target-derived neurotrophic factors regulate the death of developing forebrain neurons after a change in their trophic requirements. J Neurosci. 2001; 21:3904–3910. [PubMed: 11356878]

Mednick SA, Machon RA, Huttunen MO, Bonnett D. Adult schizophrenia following prenatal exposure to an influenza epidemic. Arch Gen Psychiatry. 1988; 45:189–192. [PubMed: 3337616]

Miller M, Christensen GE, Amit Y, Grenander U. Mathematical textbook of deformable neuroanatomies. Proc Natl Acad Sci USA. 1993; 90:11944–11948. [PubMed: 8265653]

Miller M, Banerjee A, Christensen G, Joshi S, Khaneja N, Gernander U, Matejic L. Statistical methods in computational anatomy. Stat Methods Med Res. 1997; 6:267–299. [PubMed: 9339500]

Molyneaux BJ, Arlotta P, Hirata T, Hibi M, Macklis JD. Fezl is required for the birth and specification of corticospinal motor neurons. Neuron. 2005; 47:817–831. [PubMed: 16157277]

Nielsen RE, Abitz M, Pakkenberg B. Neuron and glial cell numbers in the mediodorsal thalamic nucleus in brains of schizophrenic subjects. Image Anal Stereol. 2008; 27:133–141.

Ogren MP, Rakic P. The prenatal development of the pulvinar in the monkey: ^{3}H-thymidine autoradiographic and morphometric analyses. Anat Embryol. 1981; 162:1–20. [PubMed: 7283168]

O'Leary DDM, Borngasser D. Cortical ventricular zone progenitors and their progeny maintain spatial relationships and radial patterning during preplate development indicating an early protomap. Cereb Cortex Suppl. 2006; 1:i46–i56.

Oppenheim RW. Cell death during development of the nervous system. Ann Rev Neurosci. 1991; 14:453–501. [PubMed: 2031577]

Otake M, Schull WJ, Yoshimaru H. A review of forty-five years of study of Hiroshima and Nagasaki atomic bomb survivors. Brain damage among the prenatally exposed. J Radiat Res. 1991; 32(suppl):249–264. [PubMed: 1762113]

Pakkenberg B. Pronounced reduction of total neuron number in mediodorsal thalamic nucleus and nucleus accumbens in schizophrenics. Arch Gen Psychiatry. 1990; 47:1023–1028. [PubMed: 2241504]

Popken GJ, Bunney WE Jr, Potkin SG, Jones EG. Subnucleus-specific loss of neurons in medial thalamus of schizophrenics. Proc Natl Acad Sci, USA. 2000; 97:9276–9280. [PubMed: 10908653]

Portas CM, Goldstein JM, Shenton ME, Hokama H, Wible CG, Fischer I, Kikinis R, Donnino R, Jolesz FA, McCarley RW. Volumetric evaluation of the thalamus in schizophrenic male patients using magnetic resonance imaging. Biol Psychiatry. 1998; 43:649–659. [PubMed: 9582998]

Preuss UW, Zetzsche T, Jager M, Groll C, Frodl T, Bottlender R, Leinsinger G, Hegerl U, Hahn K, Moller HJ, Meisenzahl EM. Thalamic volume in first-episode and chronic schizophrenic subjects: a volumetric MRI study. Schizophr Res. 2005; 73:91–101. [PubMed: 15567081]

Rakic P. Neurons in the monkey visual cortex: Systematic relation between time of origin and eventual disposition. Science. 1974; 183:425–427. [PubMed: 4203022]

Rakic P. Genesis of the dorsal lateral geniculate nucleus in the rhesus monkey: Site and time of origin, kinetics of proliferation, routes of migration and pattern of distribution of neurons. J Comp Neurol. 1977a; 176:23–52. [PubMed: 409739]

Rakic P. Prenatal development of the visual system in rhesus monkey. Phil Trans R Soc Lond B. 1977b; 278:245–260. [PubMed: 19781]

Rakic P. Specification of cerebral cortical areas. Science. 1988; 241:170–176. [PubMed: 3291116]

Rakic P. Pre and post-developmental neurogenesis in primates. Clinical Neurosci Res. 2002; 2:29–39.

Rakic P, Riley KP. Regulation of axon numbers in the primate optic nerve by prenatal binocular competition. Nature. 1983; 305:135–137. [PubMed: 6888556]

Rakic P, Bourgeois JP, Eckenhoff MF, Zecevic N, Goldman-Rakic PS. Concurrent overproduction of synapses in diverse regions of the primate cerebral cortex. Science. 1986; 232:232–235. [PubMed: 3952506]

Schindler M, Wang L, Selemon LD, Goldman-Rakic PS, Rakic P, Csernansky JG. Abnormalities of thalamic volume and shape detected in fetally-irradiated rhesus monkeys with high dimensional brain mapping. Biol Psychiatry. 2002; 51:827–837. [PubMed: 12007457]

Selemon LD, Lidow MS, Goldman-Rakic PS. Increased volume and glial density in primate prefrontal cortex associated with chronic antipsychotic drug exposure. Biol Psychiatry. 1999; 46:161–172. [PubMed: 10418690]

Selemon LD, Wang L, Nebel MB, Csernansky JG, Goldman-Rakic PS, Rakic P. Direct and indirect effects of fetal irradiaton on cortical gray and white matter volume in the macaque. Biol Psychiatry. 2005; 57:83–90. [PubMed: 15607304]

Susser ES, Lin SP. Schizophrenia after prenatal exposure to the Dutch Hunger Winter of 1944–1945. Arch Gen Psychiatry. 1992; 49:983–988. [PubMed: 1449385]

Susser ES, Neugebauer R, Hoek HW, Brown AS, Lin S, Labovitz D, Gorman JM. Schizoprenia after prenatal famine. Further evidence. Arch Gen Psychiatry. 1996; 53:25–31. [PubMed: 8540774]

Tigges J, Gordon TP, McLure HM, Hall EC, Peters A. Survival rate and life span of rhesus monkeys at the Yerkes Regional Primate Research Center. Am J Primatol. 1988; 15:263–273.

Williams RW, Rakic P. Elimination of neurons from the rhesus monkey's lateral geniculate nucleus during development. J Comp Neurol. 1988; 15:424–436. [PubMed: 3417894]

Young KA, Manaye KF, Liang C-L, Hicks PB, German DC. Reduced number of mediodorsal and anterior thalamic neurons in schizophrenia. Biol Psychiatry. 2000; 47:900–953.

Young KA, Holcomb LA, Yazdani U, Hicks PB, German DC. Elevated neuron number in the limbic thalamus in major depression. Am J Psychiatry. 2004; 161:1270–1277. [PubMed: 15229061]

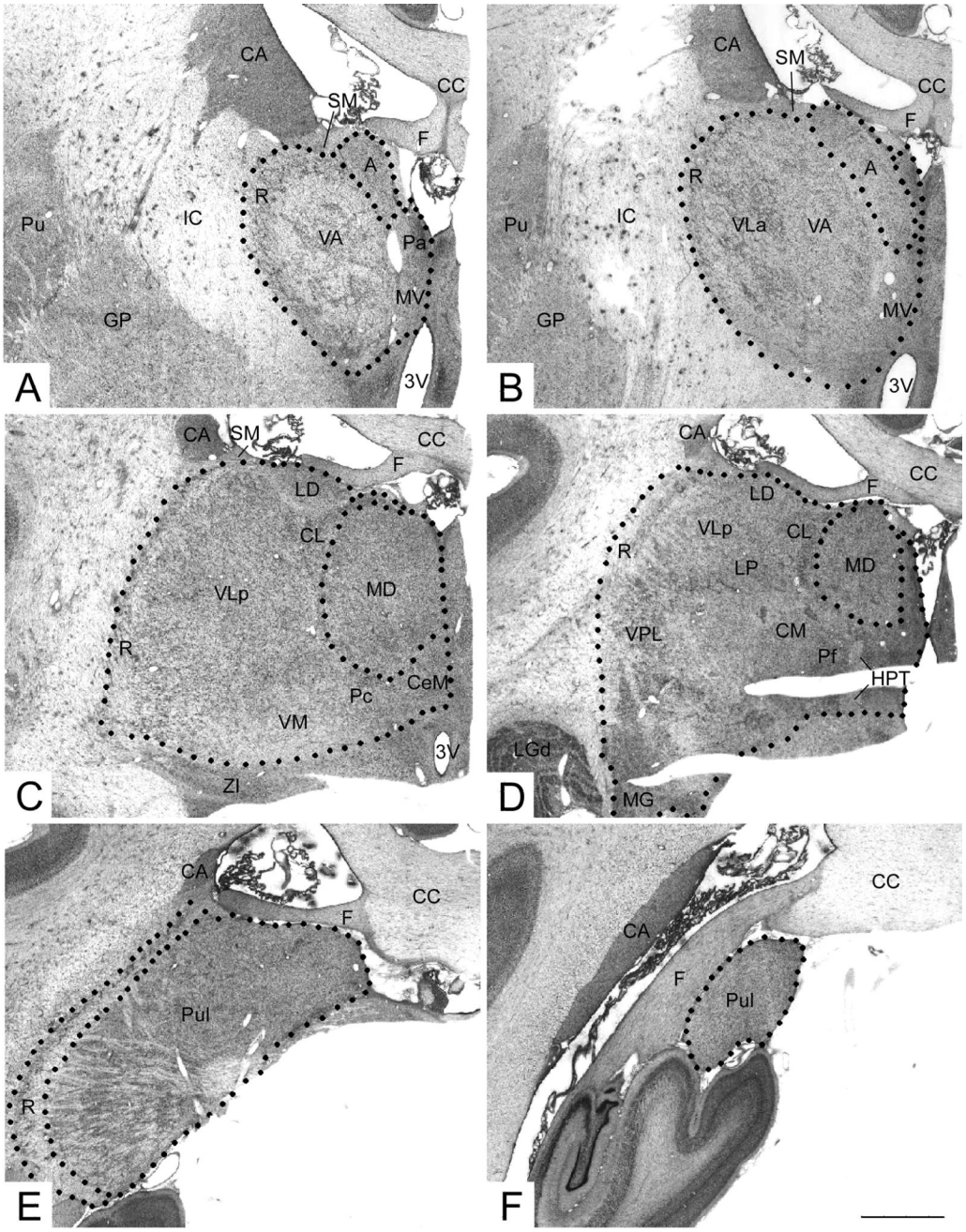

Figure 1.

Photomicrographs of the thalamus. The boundaries of thalamic nuclei examined in this study are shown: A,B the anterior nucleus (A) including both dorsal and ventral subdivisions; C, D, the mediodorsal nucleus (MD); and E,F, the pulvinar nucleus (Pul). See separate page for a complete list of abbreviations. Scale bar = 1 mm.

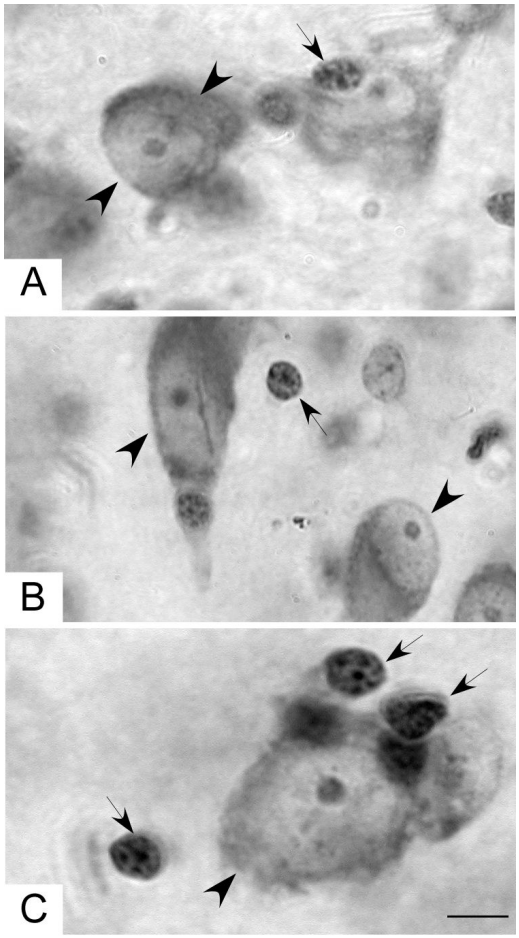

Figure 2.
High power photomicrographs illustrating typical neurons (large arrowheads) and glia (small arrows): A, the anterior nucleus, B the mediodorsal nucleus, and C the pulvinar nucleus. Scale bar = 5 μm.

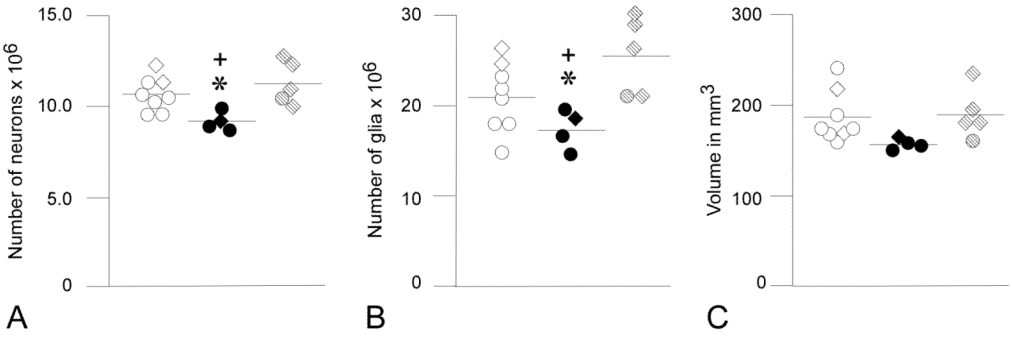

Figure 3.

Graphs showing (A) total number of neurons, (B) total number of glia and (C) volume of the whole thalamus. Values for CONs are indicated by open circles (adults) and open diamonds (infants), eFIMs by solid circles (adults) and solid diamonds (infants), and mFIMs by stippled circles (adults) and stippled diamonds (infants). Means shown have not been adjusted for differences in age. Total number of neurons in the whole thalamus was reduced in the eFIMs in comparison to CONs ($p= 0.02^{*}$) and to mFIMs ($p= 0.025^{+}$). Total number of glial cells in eFIMs was also reduced compared to the other two groups (vs CONs, $p= 0.037^{*}$; vs. mFIMs, $p= 0.014^{+}$). There were no significant differences in volume among the three groups.

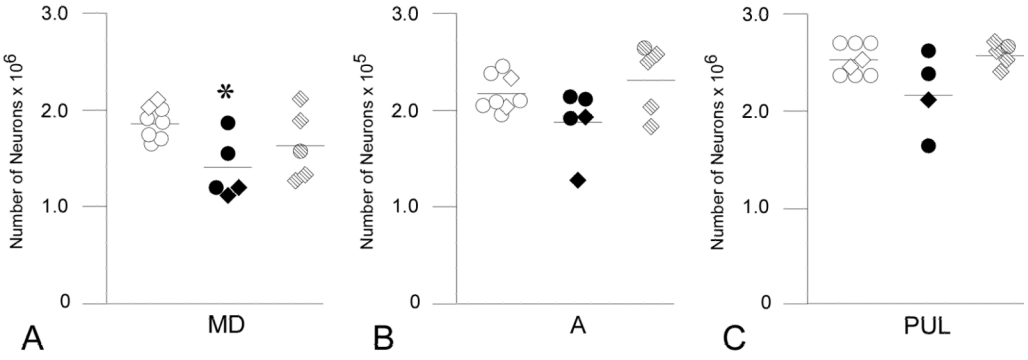

Figure 4.

Total number of neurons in the (A) mediodorsal (MD), (B) anterior (A), and (C) pulvinar (PUL) nuclei. Neuronal number MD was reduced in eFIMs (adults= solid circles, infants= solid diamonds) in comparison to CONs (adults= open circles, infants= open diamonds; p= 0.034*). Mean bars have not been adjusted for age. Number of neurons in MD in the mFIM group (adults= stippled circles, infants= stippled diamonds) did not differ from that of the CONs or eFIMS. There were no differences in total number of neurons among the three groups in the anterior or pulvinar nuclei.

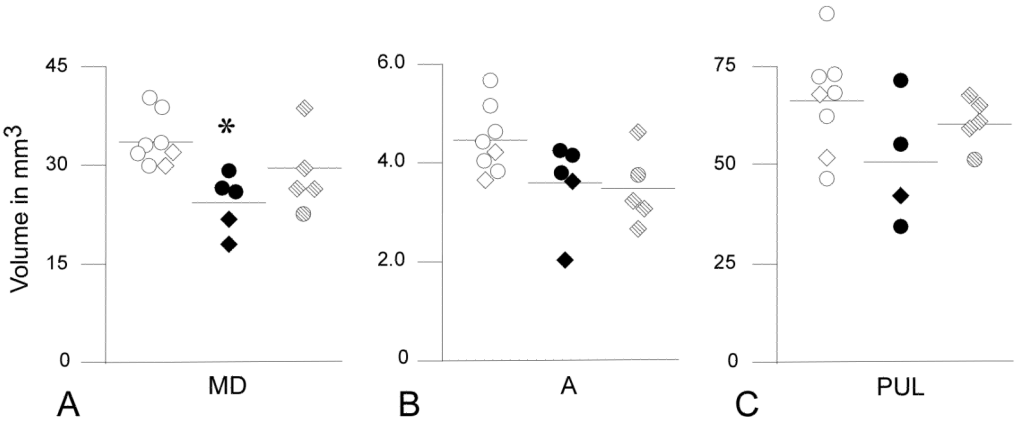

Figure 5.

Volume of the (A) mediodorsal (MD), (B) anterior (A), and (C) pulvinar (PUL) nuclei. Volume of MD was reduced in eFIMs (adults= solid circles, infants= solid diamonds) in comparison to CONs (adults= open circles, infants= open diamonds, p= 0.018*) but did not differ from that of mFIMs (adults= stippled circles, infants= stippled diamonds). MD volume was similar in CONs and mFIMs. There were no significant differences among the three groups in volume of the anterior or pulvinar nuclei. Unadjusted means are shown.

Table 1

Irradiation Exposure and Dose

Animal	Sex	Age (yrs)	Time in embryonic day (E) and dose of irradiation (in cGy)	Total dose in cGy
CON1	M	9.42		0
CON2	F	14.17		0
CON3	F	12.42		0
CON4	F	10.00		0
CON5	F	7.58		0
CON6	F	4.83		0
CON7	M	.17		0
CON8	F	.17		0
eFIM1	M	7.75	E33(25), E35(50), E37(50), E41(50)	175
eFIM2	M	6.42	E33(50), E35(50), E36(50), E37(50)	200
eFIM3	F	9.17	E35(50), E37(50), E39(50), E42(50)	200
eFIM4	M	.33	E33(50), E35(50), E38(50), E40(50)	200
eFIM5	F	.33	E33(50), E35(50), E38(50), E40(50)	200
mFIM1	M	9.75	E73(100), E74(100), E75(100)	300
mFIM2	M	1.50	E70(50), E72(50), E74(50), E77(50), E79(50), E81(50), E84(50)	350
mFIM3	M	.18	E80(50), E83(50), E86(50), E88(50), E90(50)	250
mFIM4	F	.17	E79(100), E81(100), E83(100)	300
mFIM5	F	.18	E70(63), E72(63), E75(50), E77(50), E79(50)	276

Table 2

Total Cell Number and Volume Data

Group	Neurons (SE)	Glia (SE)	Volume in mm^3 (SE)
Adjusted Group Means*			
Whole Thalamus			
CON	10.8×10^6 (0.31×10^6)	22.0×10^6 (0.92×10^6)	190 (9)
eFIM	9.1×10^6 (0.42×10^6)*a*	17.5×10^6 (1.25×10^6)*a*	160 (13)
mFIM	10.9×10^6 (0.41×10^6)*b*	23.5×10^6 (1.21×10^6)*b*	180 (12)
Mediodorsal nucleus			
CON	1.87×10^6 (0.11×10^6)	3.57×10^6 (0.29×10^6)	35 (2)
eFIM	1.39×10^6 (0.13×10^6)*a*	2.59×10^6 (0.35×10^6)	25 (2)*a*
mFIM	1.62×10^6 (0.13×10^6)	2.90×10^6 (0.38×10^6)	30 (2)
Anterior nucleus			
CON	2.13×10^5 (0.11×10^5)	3.82×10^5 (0.26×10^5)	4.4 (0.3)
eFIM	1.88×10^5 (0.13×10^5)	3.25×10^5 (0.32×10^5)	3.6 (0.3)
mFIM	2.36×10^5 (0.14×10^5)	3.87×10^5 (0.34×10^5)	3.6 (0.4)
Pulvinar nucleus			
CON	2.50×10^6 (0.09×10^6)	4.60×10^6 (0.29×10^6)	66 (5)
eFIM	2.18×10^6 (0.12×10^6)	4.35×10^6 (0.40×10^6)	50 (6)
mFIM	2.60×10^6 (0.11×10^6)	4.59×10^6 (0.38×10^6)	61 (6)
Unadjusted Group Means			
Whole Thalamus			
CON	10.6×10^6 (0.94×10^6)	20.9×10^6 (3.87×10^6)	187 (29)
eFIM	9.1×10^6 (0.49×10^6)	17.3×10^6 (2.15×10^6)	157 (7)
mFIm	11.2×10^6(1.16×10^6)*b*	25.5×10^6 (4.37×10^6)*b*	190 (29)
Mediodorsal Nucleus			
CON	1.86×10^6 (1.66×10^5)	3.44×10^6 (8.33×10^5)	35 (4)
eFIM	1.39×10^6 (3.21×10^5)*a*	2.61×10^6 (6.66×10^5)	25 (5)*a*
mFIM	1.63×10^6 (3.60×10^5)	3.07×10^6 (9.13×10^5)	30 (6)
Anterior Nucleus			
CON	1.76×10^5 (0.30×10^5)	2.94×10^5 (0.43×10^5)	4.5 (0.7)
eFIM	1.43×10^5 (0.36×10^5)	2.52×10^5 (0.89×10^5)	3.6 (0.9)
mFIM	1.98×10^5 (0.28×10^5)*b*	3.07×10^5 (0.59×10^5)	3.5 (0.8)
Pulvinar Nucleus			
CON	2.52×10^6 (0.16×10^6)	4.61×10^6 (0.55×10^6)	66 (13)
eFIM	2.18×10^6 (0.42×10^6)	4.35×10^6 (1.31×10^6)	51 (16)
mFIM	2.57×10^6 (0.11×10^6)	4.58×10^6 (0.46×10^6)	60 (6)

*adjusted for age

a= eFIM vs CON, $p < 0.05$

^{b}= eFIM vs mFIM, $p < 0.05$